Nanoscale

COMMUNICATION

View Article Online
View Journal | View Issue

Cite this: *Nanoscale*, 2019, **11**, 19297

Received 22nd July 2019,
Accepted 9th September 2019

DOI: 10.1039/c9nr06239d

rsc.li/nanoscale

A facile synthetic approach to nanostructured Li_2S cathodes for rechargeable solid-state Li–S batteries†

Hany El-Shinawi, *[a] Edmund J. Cussen[b] and Serena A. Corr *[a]

Li–S solid state batteries, employing Li_2S as a pre-lithiated cathode, present a promising low cost, high capacity and safer alternative to their liquid electrolyte counterparts, where dissolution of intermediate polysulfide species can result in loss of active material and a subsequent decrease in ionic conductivity. A nanostructured Li_2S material would afford greater flexibility in optimising the cathode composite for more harmonious electrode–electrolyte interactions, yet facile routes to such nanoscale materials are limited. Here, we report a facile and scalable microwave approach to directly synthesize nanostructured Li_2S from a glyme solution containing lithium polysulfides. As-synthesized Li_2S presents an ideal architecture for the construction of free-standing cathodes for all-solid-state Li–S batteries.

Reversible electrochemical lithiation of S to Li_2S in rechargeable Li–S batteries is a promising approach to realizing low-cost, high energy density batteries.[1] Abundant, light-weight sulfur offers a potential specific capacity of 1672 mA h g^{-1} which, at an order of magnitude higher than that provided by conventional intercalation-type cathodes such as $LiCoO_2$ and $LiFePO_4$, makes Li–S batteries suitable for high energy storage applications such as powering electric vehicles.[1,2] Li_2S has been suggested as a pre-lithiated cathode, negating the necessity of metallic lithium as an anode.[2,3] With the application of a solid-electrolyte, further advantages such as higher ionic conductivities and potentially mitigating deleterious polysulfide shuttle activity are possible.[4–6] However, a serious bottleneck in the widespread uptake of such a pre-lithiated material has been the limited synthetic routes to Li_2S. Preferably, Li_2S would be composited with an electronic conductor and a Li-ion conducting medium on the nanoscale to promote greater electrode–electrolyte interactions, in an architecture that would accommodate the volume changes associated with cycling. The application of nanostructured Li_2S also Recent years have seen efforts made in developing novel Li_2S composites, for example in combination with carbon and/or solid electrolyte.[3] A significant benefit to the community would be a reliable and scalable synthetic route to nanostructured Li_2S, which up to now has been limited and in several cases complicated and costly. Reported routes include impregnating carbon materials with ethanolic solutions of commercial Li_2S,[7–16] chemical reaction of sulfur with lithium triethylborohydride or stabilized lithium metal powder,[4,17–23] carbon-based reduction of Li_2SO_4 and polysulfides,[24–30] reactions between H_2S and lithium naphthalenide,[31] and burning Li foils in a CS_2 vapour.[32] Thus, there remains a lack of facile routes to Li_2S which are scalable and afford control over the final particle morphology and size. Here we report the synthesis of nanostructured Li_2S, prepared by a simple microwave approach, together with its performance in an all solid-state Li–S battery. Our results demonstrate that nanostructured Li_2S employed within a free-standing cathode displays exceptional cycling stability, achieving capacities of 440 mA h g^{-1} at cycling rates of 100 μA cm^{-2} up to 400 cycles.

Nanostructured Li_2S is prepared using a simple 20-minute microwave-assisted heat treatment of a tetraglyme solution containing elemental sulfur and lithium *tert*-butoxide, at temperatures as low as 200 °C (see ESI for experimental details†). X-ray diffraction patterns of this microwave-synthesised Li_2S powder (Fig. 1) reveal peak broadening consistent with a reduction in particle size (with an estimated crystallite size of 10 nm from Scherrer broadening), compared to a commercial Li_2S sample (Sigma Aldrich, 99.98%). All peaks could be indexed to the cubic lattice of the antifluorite structure of Li_2S. Nanoparticles of Li_2S are confirmed by scanning electron microscopy (SEM) images, were aggregates of particles are observed. Fig. 2 illustrates the importance of the S/lithium *tert*-butoxide concentration ratio on the resulting particle size and distribution, with three examples shown (see Fig. S1† for

[a]*Department of Chemical and Biological Engineering, University of Sheffield, Sir Robert Hadfield Building, Sheffield, S1 3JD, UK. E-mail: s.a.corr@sheffield.ac.uk*
[b]*Department of Materials Science and Engineering, University of Sheffield, Sir Robert Hadfield Building, Sheffield, S1 3JD, UK*

†Electronic supplementary information (ESI) available. See DOI: 10.1039/c9nr06239d

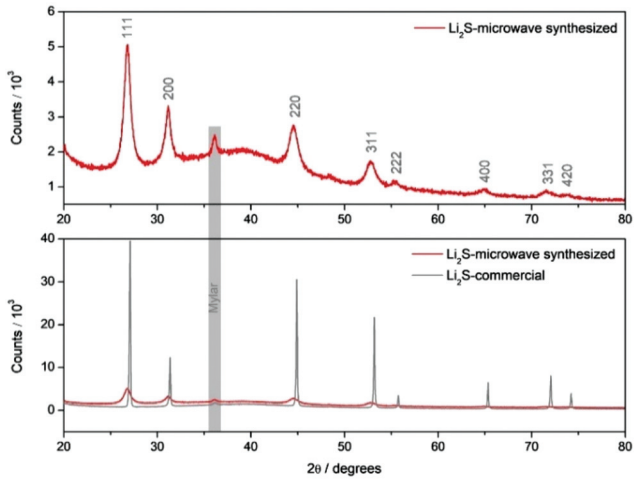

Fig. 1 XRD patterns of commercial Li_2S and microwave-synthesized Li_2S (0.15 M sulfur solution). An air tight sample holder employing a Mylar window was employed.

further SEM images). Our experiments reveal that Li_2S prepared using 0.15 M sulfur solution gave particles with the smallest size and narrowest size distribution.

Such nanostructured material provides a promising electrode architecture in terms of providing shorter pathlengths for Li-ion transport, as well as larger electrode–electrolyte contact areas, compared with bulk materials and this sample was selected for further electrochemical study.

It has been previously observed that conductive thin layers of Li_3PS_4 can be deposited from a THF solution containing Li_2S and P_2S_5.[4,33] Here, we followed a modified approach to incorporate our microwave-synthesized nanostructured Li_2S in a three-phase Li_3PS_4/nano-Li_2S/C nanocomposite. Firstly, nanostructured carbon black is composited with P_2S_5 using a melt-diffusion technique (Fig. S2†) before mixing with microwave-synthesized Li_2S in THF (molar ratio of P_2S_5 : Li_2S is 1 : 20) to produce the final Li_3PS_4/Li_2S/C nanocomposite. This corresponds to 40 wt% Li_2S in the composite. Characterisation of the final composite by SEM, EDX and XRD are shown in Fig. 3. EDX analysis reveals a homogeneous phosphorus and sulfur distribution across the material, while the presence of Li_3PS_4 is not evident from XRD nor from SEM (pure β-Li_3PS_4 has a distinctive morphology of micron-sized, porous brick-shaped particles). These data suggest the formation of a thin film of Li_3PS_4, which is either amorphous or is formed on a much shorter length scale not detectable by Bragg diffraction. The formation of a Li_3PS_4 thin coating on the Li_2S/C surface is

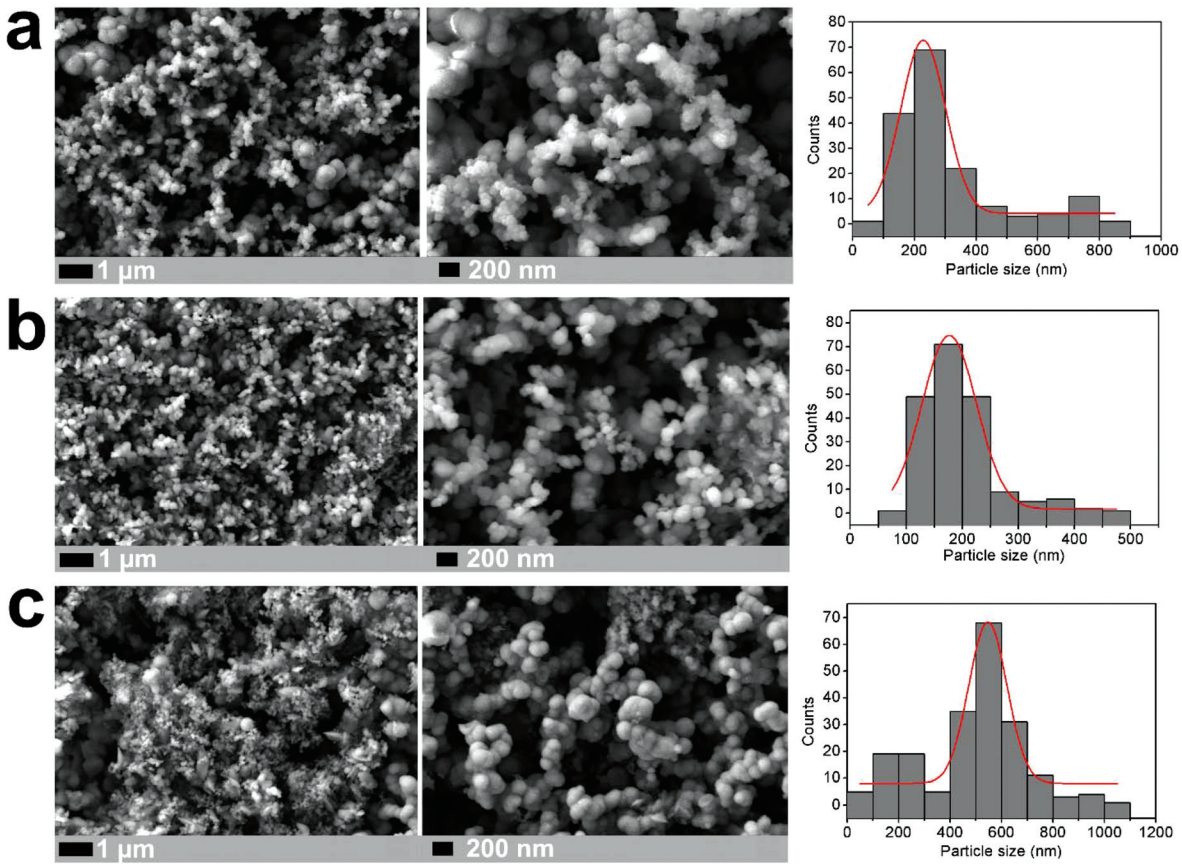

Fig. 2 Morphology and particle size distributions based on SEM (N = 170) of Li_2S prepared from (a) 0.075 M, (b) 0.15 M and (c) 0.3 M sulfur solutions. The mean particle sizes are given as 228 (±72) nm, 177 (±49) nm and 546 (±74) nm respectively.

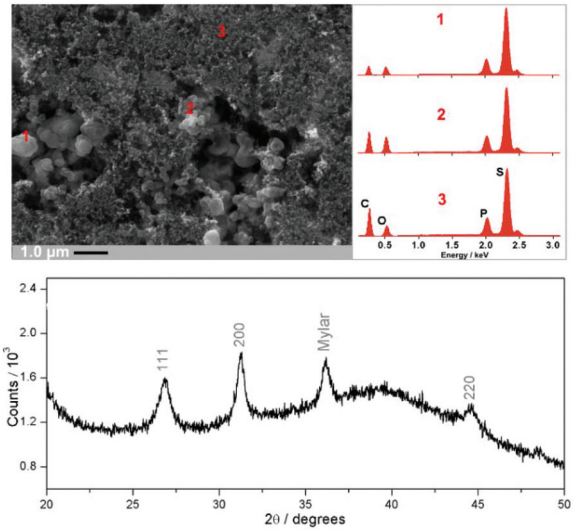

Fig. 3 SEM/EDX analysis and XRD pattern of the as-synthesized Li_3PS_4/Li_2S/C composite.

consistent with previous reports.[4] This is further confirmed by performing the control experiment, in which a P_2S_5-rich/C composite is mixed with Li_2S (molar ratio of P_2S_5 : Li_2S is 1 : 10). In addition to formation of bulk β-Li_3PS_4, which is confirmed by XRD and SEM (Fig. S3†), a homogeneous distribution of P and S is also observed across this material indicating the formation again of a thin coating of Li_3PS_4.

An all-solid-state battery was prepared using the Li_3PS_4/Li_2S/C nanocomposite as a free-standing cathode, β-Li_3PS_4 as the solid electrolyte and metallic lithium as the anode. These components were pressed together under 2 tons of pressure, employing Al and Ni foils to support and collect the current from the cathode and the anode, respectively (Fig. 4a, insert). The cell cycled at 60 °C and at current densities ranging between 20 and 100 μA cm^{-2} for up to 400 cycles (corresponding to ~ C/2 and C/10). Fig. 4a shows the typical charge and discharge profiles of the battery at 20 μA cm^{-2}. In addition to retaining the capacity, it is notable that the voltage profiles comprise well-defined discharge and charge plateaus, displaying small potential hysteresis. We attribute this small hysteresis to improved electronic and ionic conductivities of the composite cathode and a reduced interfacial resistance at the solid-electrolyte/cathode interface, as illustrated by impedance spectroscopy measurements (see below). Increasing the discharge/charge rate from 20 to 100 μA cm^{-2} reduced the capacity from ~ 840 to ~ 440 mA h g^{-1}, but this capacity is retained over more than 300 additional cycles with coulombic efficiency close to 100% (Fig. 4b). Fig. S4† displays SEM images of the Li_3PS_4/Li_2S/C electrode before and after cycling revealing no obvious change of the morphology after 410 cycles at different rates. Some surface cracks are observed which can be attributed to volume changes during cycling; importantly, these cracks do not lead to a loss of contact between the electrode domains or to delamination of the electrode and the solid electrolyte. Impedance measurements prior to and after cycling, indicated an increase of the resistance of the cell from ~250 Ω to ~600 Ω after 410 cycles at different rates (Fig. S5†). This limited growth of cell resistance with long-term cycling is consistent with capacity retention and maintaining electrode integrity and suggests good stability of the solid-electrolyte/cathode interface. For comparison, in a recent study on Li_6PS_5Cl–Li_2S all-solid-state batteries, a cycled battery employing Li_2S/C as the cathode exhibited an interfacial resistance that is one order of magnitude higher than the resistance of the fresh cell after only 37 cycles.[34]

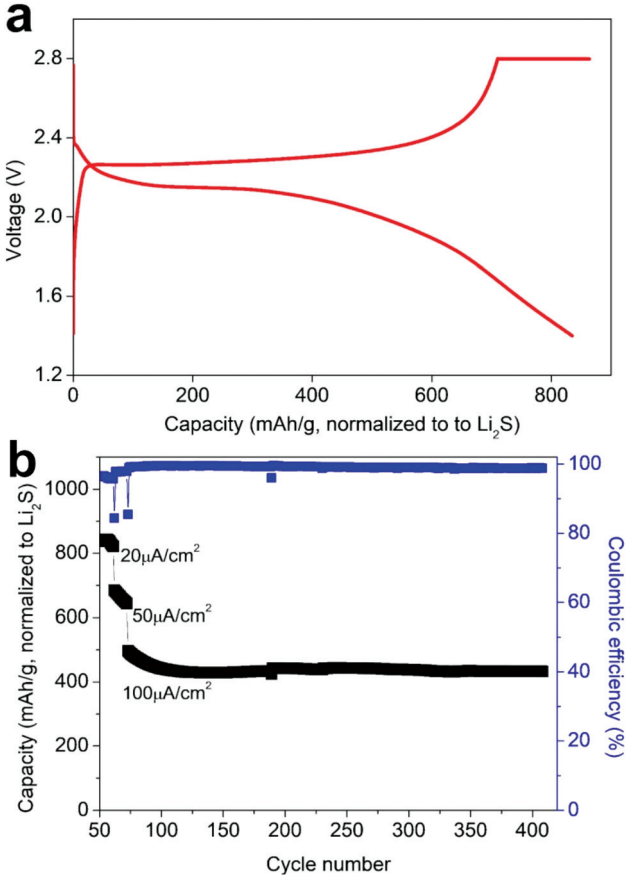

Fig. 4 (a) Typical charge/discharge profile of the all-solid-state battery at 20 μA cm^{-2} current density. (b) Cycle performance of the battery at current densities of 20, 50 and 100 μA cm^{-2} over 400 cycles.

Conclusions

In summary, we demonstrate that nanostructured Li_2S can be prepared by a simple, fast, microwave heat treatment of a glyme solution containing lithium polysulfides. The as-synthesized Li_2S presents an ideal architecture for the construction of free-standing cathodes comprising Li_3PS_4/Li_2S/C nanocomposites. Crucially, this synthetic approach is highly reproducible, having been repeated numerous times, and scalable. The performance of this nanostructured Li_2S as a cathode in

an all-solid-state battery demonstrates excellent capacity retention at current densities of up to 100 μA cm^{-2}, with limited increases in cell resistance and close to 100% coulombic efficiencies, which we attribute to increased electrode–electrolyte contact area and shorter Li^+ diffusion pathlengths.

Conflicts of interest

There are no conflicts to declare.

Acknowledgements

We gratefully acknowledge the support of the University of Sheffield in our research. Our work was supported by the EPSRC [EP/N001982/2] and the ISCF Faraday Challenge project "SOLBAT – The Solid-State (Li or N (a) Metal-Anode Battery" [grant number FIRG007].

Notes and references

1 (*a*) P. G. Bruce, S. A. Freunberger, L. J. Hardwick and J. M. Tarascon, *Nat. Mater*, 2012, **11**, 19; (*b*) S.-K. Lee, Y. J. Lee and Y. K. Sun, *J. Power Sources*, 2016, **323**, 174.
2 A. Manthiram, Y. Fu, S.-H. Chung, C. Zu and Y.-S. Su, *Chem. Rev.*, 2014, **114**, 11751.
3 D. Su, D. Zhou, C. Wang and G. Wang, *Adv. Funct. Mater.*, 2018, **28**, 1800154.
4 Z. Lin, Z. C. Liu, N. J. Dudney and C. D. Liang, *ACS Nano*, 2013, **7**, 2829.
5 F. Han, J. Yue, X. Fan, T. Gao, C. Luo, Z. Ma, L. Suo and C. Wang, *Nano Lett.*, 2016, **16**, 4521.
6 Z. Jiao, L. Chena, J. Si, C. Xu, Y. Jiang, Y. Zhu, Y. Yang and B. Zhao, *J. Power Sources*, 2017, **353**, 167.
7 F. Wu, H. Kim, A. Magasinski, J. T. Lee, H.-T. Lin and G. Yushin, *Adv. Energy Mater.*, 2014, **4**, 1400196.
8 F. Wu, A. Magasinski and G. Yushin, *J. Mater. Chem. A*, 2014, **2**, 6064.
9 C. Wang, X. Wang, Y. Yang, A. Kushima, J. Chen, Y. Huang and J. Li, *Nano Lett.*, 2015, **15**, 1796.
10 M. Wu, Y. Cui and Y. Fu, *ACS Appl. Mater. Interfaces*, 2015, **7**, 21479.
11 F. Wu, J. T. Lee, F. Fan, N. Nitta, H. Kim, T. Zhu and G. Yushin, *Adv. Mater.*, 2015, **27**, 5579.
12 Y. Qiu, G. Rong, J. Yang, G. Li, S. Ma, X. Wang, Z. Pan, Y. Hou, M. Liu, F. Ye, W. Li, Z. W. Seh, X. Tao, H. Yao, N. Liu, R. Zhang, G. Zhou, J. Wang, S. Fan, Y. Cui and Y. Zhang, *Adv. Energy Mater.*, 2015, **5**, 1501369.
13 G. Zhou, E. Paek, G. S. Hwang and A. Manthiram, *Adv. Energy Mater.*, 2016, **6**, 1501355.
14 J. He, Y. Chen, W. Lv, K. Wen, C. Xu, W. Zhang, W. Qin and W. He, *ACS Energy Lett.*, 2016, **1**, 820.
15 F. Wu, J. T. Lee, E. Zhao, B. Zhang and G. Yushin, *ACS Nano*, 2016, **10**, 1333.
16 D. H. Wang, D. Xie, T. Yang, Y. Zhong, X. L. Wang, X. H. Xia, C. D. Gu and J. P. Tu, *J. Power Sources*, 2016, **313**, 233.
17 J. A. Gladysz, V. K. Wong and B. S. Jick, *Tetrahedron*, 1979, **35**, 2329.
18 Z. Lin, C. Nan, Y. Ye, J. Guo, J. Zhu and E. J. Cairns, *Nano Energy*, 2014, **9**, 408.
19 K. Zhang, L. Wang, Z. Hu, F. Cheng and J. Chen, *Sci. Rep.*, 2014, **4**, 6467.
20 C. Nan, Z. Lin, H. Liao, M. K. Song, Y. Li and E. J. Cairns, *J. Am., Chem. Soc.*, 2014, **136**, 4659.
21 Y. Hwa, J. Zhao and E. J. Cairns, *Nano Lett.*, 2015, **15**, 3479.
22 L. Suo, Y. Zhu, F. Han, T. Gao, C. Luo, X. Fan, Y.-S. Hu and C. Wang, *Nano Energy*, 2015, **13**, 467.
23 S. Zheng, Y. Chen, Y. Xu, F. Yi, Y. Zhu, Y. Liu, J. Yang and C. Wang, *ACS Nano*, 2013, **7**, 10995.
24 Z. Yang, J. Guo, S. K. Das, Y. Yu, Z. Zhou, H. D. Abruña and L. A. Archer, *J. Mater. Chem. A*, 2013, **1**, 1433.
25 Z. Li, S. Zhang, C. Zhang, K. Ueno, T. Yasuda, R. Tatara, K. Dokko and M. Watanabe, *Nanoscale*, 2015, **7**, 14385.
26 J. Zhang, Y. Shi, Y. Ding, L. Peng, W. Zhang and G. Yu, *Adv. Energy Mater.*, 2017, **7**, 1602876.
27 M. Yu, Z. Wang, Y. Wang, Y. Dong and J. Qiu, *Adv. Energy Mater*, 2017, 1700018.
28 F. Ye, H. Noh, J. Lee, H. Lee and H.-T. Kim, *J. Mater. Chem. A*, 2018, **6**, 6617.
29 Y. Fu, C. Zu and A. Manthiram, *J. Am. Chem. Soc.*, 2013, **135**, 18044.
30 M. Kohl, J. Brückner, I. Bauer, H. Althues and S. Kaskel, *J. Mater. Chem. A*, 2015, **3**, 16307.
31 X. M. Li, C. A. Wolden, C. M. Ban and Y. G. Yang, *ACS Appl. Mater. Interfaces*, 2015, **7**, 28444.
32 G. Tan, R. Xu, Z. Xing, Y. Yuan, J. Lu, J. Wen, C. Liu, L. Ma, C. Zhan and Q. Liu, *Nat. Energy*, 2017, **2**, 17090.
33 H.-D. Lim, H.-K. Lim, X. Xing, B.-S. Lee, H. Liu, C. Coaty, H. Kim and P. Liu, *Adv. Mater. Interfaces*, 2018, **5**, 1701328.
34 C. Yu, S. Ganapathy, N. J. J. de Klerk, I. Roslon, E. R. H. van Eck, A. P. M. Kentgens and M. Wagemaker, *J. Am. Chem. Soc.*, 2016, **138**, 11192.

